Disruptive *SCYL1* Mutations Underlie a Syndrome Characterized by Recurrent Episodes of Liver Failure, Peripheral Neuropathy, Cerebellar Atrophy, and Ataxia

Wolfgang M. Schmidt,[1,7] S. Lane Rutledge,[2,7] Rebecca Schüle,[3,4,5,7] Benjamin Mayerhofer,[1] Stephan Züchner,[5] Eugen Boltshauser,[6] and Reginald E. Bittner[1,*]

Hereditary ataxias comprise a group of genetically heterogeneous disorders characterized by clinically variable cerebellar dysfunction and accompanied by involvement of other organ systems. The molecular underpinnings for many of these diseases are widely unknown. Previously, we discovered the disruption of *Scyl1* as the molecular basis of the mouse mutant *mdf*, which is affected by neurogenic muscular atrophy, progressive gait ataxia with tremor, cerebellar vermis atrophy, and optic-nerve thinning. Here, we report on three human individuals, from two unrelated families, who presented with recurrent episodes of acute liver failure in early infancy and are affected by cerebellar vermis atrophy, ataxia, and peripheral neuropathy. By whole-exome sequencing, compound-heterozygous mutations within *SCYL1* were identified in all affected individuals. We further show that in SCYL1-deficient human fibroblasts, the Golgi apparatus is massively enlarged, which is in line with the concept that SCYL1 regulates Golgi integrity. Thus, our findings define *SCYL1* mutations as the genetic cause of a human hepatocerebellar neuropathy syndrome.

Hereditary cerebellar ataxias are genetically heterogeneous disorders characterized by clinically variable gait disturbances and often accompanied by additional neurological symptoms and involvement of other organs. The molecular underpinnings of the vast majority of these disorders still remain widely unknown.[1–4] In a previous study, we uncovered the genetic defect underlying the *mdf* (muscle deficient) mouse by identifying a frame-shifting mutation in *Scyl1*[5]. Initially, the *mdf* mouse was considered a murine motor-neuron-disease model, owing to the progressive loss of motor neurons in the spinal cord and brain stem, causing severe neurogenic muscular atrophy.[6] Our group refined the *mdf* phenotype by demonstrating that the *mdf* mouse is affected by a complex form of spinocerebellar ataxia, characterized by progressive gait ataxia, cerebellar vermis atrophy, Purkinje cell loss, and optic-nerve thinning.[5]

SCYL1 is highly conserved among eukaryotes and belongs to the SCY1-like family of catalytically inactive protein kinases, harboring an N-terminal serine-threonine kinase-like domain,[7] a centrally located HEAT repeat domain, and C-terminal protein-interaction motifs. Recent findings by others have demonstrated that SCYL1 represents an important protein at the interface between the Golgi apparatus and the membrane trafficking machinery mediated by coatomer (COPI)-coated vesicles.[8–10] Specifically, it has been shown that SCYL1 exerts a crucial role in COPI-mediated retrograde protein trafficking by undergoing oligomerization through the HEAT repeats and interacting with several key components of COPI coats.[8] In addition, SCYL1 is a cytoplasmic component of the nuclear tRNA export machinery.[11] Together, this suggests that SCYL1 is involved in vital intracellular transport processes, which might provide a basis for understanding the molecular mechanism underlying disease states caused by loss of SCYL1.

Here, we report on two families with three individuals affected by a previously undescribed ataxia syndrome. Informed consent was obtained from all involved individuals (or their parents), and the institutional ethical committees of the participating medical centers (University of Alabama at Birmingham and the University of Miami) approved the study.

First, we identified two siblings, a young woman (20 years old, F1:II.2) and her brother (16 years old, F2:II.3), born to unrelated healthy parents of white European descent with British and German roots (family 1), with a strikingly similar clinical phenotype (Table 1). Beginning at the age of 9 months, both siblings presented with recurrent episodes of liver failure mainly triggered by fever. These recurrent and occasionally severe episodes ceased in mid-childhood. However, both were left with chronic residual fibrotic liver disease and pronounced hepatomegaly and concomitant splenomegaly (Figure 1). Neurologically, both siblings had a delay in achieving early motor milestones. Since early childhood, they developed cerebellar dysfunction presenting as gait disturbances (inability to tandem gait, mild balance difficulties, occasional falling) and intention tremor. Additionally, they developed muscle weakness restricted to their lower legs,

[1]Neuromuscular Research Department, Center of Anatomy and Cell Biology, Medical University of Vienna, 1090 Vienna, Austria; [2]Department of Genetics, University of Alabama at Birmingham, Birmingham, AL 35294, USA; [3]Department of Neurodegenerative Diseases, Hertie-Institute for Clinical Brain Research, University of Tübingen, 72076 Tübingen, Germany; [4]German Research Center for Neurodegenerative Diseases, University of Tübingen, 72076 Tübingen, Germany; [5]Dr. John T. Macdonald Department of Human Genetics and John P. Hussman Institute for Human Genomics, Miller School of Medicine, University of Miami, Miami, FL 33136, USA; [6]Division of Pediatric Neurology, University Children's Hospital, 8032 Zurich, Switzerland
[7]These authors contributed equally to this work
*Correspondence: reginald.bittner@meduniwien.ac.at
http://dx.doi.org/10.1016/j.ajhg.2015.10.011.

Table 1. Genetic and Clinical Findings of Individuals with *SCYL1* Mutations

	Family 1		Family 2
	Individual 1 (F1:II.2)	**Individual 2 (F1:II.3)**	**Individual 3 (F2:II.1)**
Age at most recent clinical examination (years)	20	16	17
Gender	female	male	female
Descent	European		Cuban
SCYL1 mutation allele 1	c.937delG, p.Val313Cysfs*6		c.1230+1G>A, p.?
SCYL1 mutation allele 2	c.1509_1510delTG, p.Ala504Profs*15		c.1636C>T, p.Gln546*
Hepatology			
No. of recurrent episodes of liver dysfunction (age at first episode to age at last episode)	5 (9 months to 11 years)	3 (9 months to 6 years)	3 (18 months to 3 years)
Hepatosplenomegaly	++	++	+
Liver biopsy: focal bridging fibrosis	+	ND	+
Neurology			
Walking independently (months)	17	24	12
Cognition	normal	mild intellectual disability	mild learning disability
Neurogenic stutter (age of onset, years)	+ (20)	++ (4)	++ (3)
Cerebellar oculomotor disturbance	+	+	saccadic pursuit
Limb ataxia (UL/LL)	−/−	−/−	+/+
Gait ataxia (onset)	+ (early childhood)	+ (early childhood)	+ (childhood)
Distal weakness	LL > UL	LL > UL	LL > UL
Muscle atrophy	LL = UL	LL = UL	LL = UL
Sensory deficits and symptoms	decreased pain perception (distal LL)	ND	intermittent distal paresthesias (UL and LL)
Electroneurophysiology	ND	ND	axonal PNP
Stretch reflexes	decreased (LL)	decreased (LL)	increased (UL > LL)
Spasticity	−	−	+ (UL)
Hip abductor weakness	−	−	+ (LL, central pattern)
Tremor	intention (cerebellar)	intention (cerebellar)	action
MRI			
Cerebellar vermis atrophy	++	++	+
Optic nerve thinning	+	+	ND

Abbreviations are as follows: UL, upper limbs; LL, lower limbs; PNP, peripheral neuropathy; ND, not determined; −, not present; +, present (mild); ++, present (pronounced).

presenting with foot drop, and numbness, indicative of a hereditary motor and sensory neuropathy. Both individuals are affected by neurogenic stuttering, which is more pronounced in the male sibling, negatively impacting his communication skills (Table 1).

Initial MRI scans were performed at ages 9 (F1:II.3) and 13 years (F1:II.2), respectively, and revealed a selective atrophy of the cerebellar vermis (Figures 2A–2C), which was apparently non-progressive over a follow-up period of 7 years. The hemispheres of the cerebellum appeared normal (Figure 2C). Additionally, thinning of the optic nerves (Figure 2D) was depicted on MRI scans performed at ages 16 (F1:II.3) and 20 (F1:II.2), compatible with subclinical optic atrophy given that both individuals still have well-preserved visual acuity. In the first MRI, measurements of the optic nerves were not possible due to artifacts caused by dental braces.

To unravel the genetic etiology of the cerebellar ataxia syndrome in this family, we performed whole-exome sequencing.[13–15] DNA libraries were constructed from one affected individual (F1:II.3), both parents (F1.I.1 and F1:I.2), and the unaffected sister (F1:II.1) with the

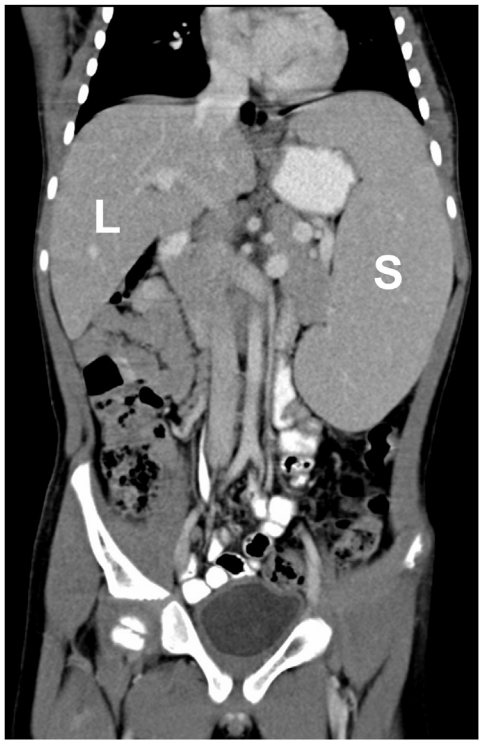

Figure 1. Hepato- and Splenomegaly Represent Early-Onset Clinical Findings
Abdominal computed tomography image (coronal reconstruction) showing significant hepato- and splenomegaly in the male affected individual (family 1) at age 8 years. The liver (L) was palpable 9 cm below the right costal margin and the spleen (S) was palpable 6 cm below the left costal margin.

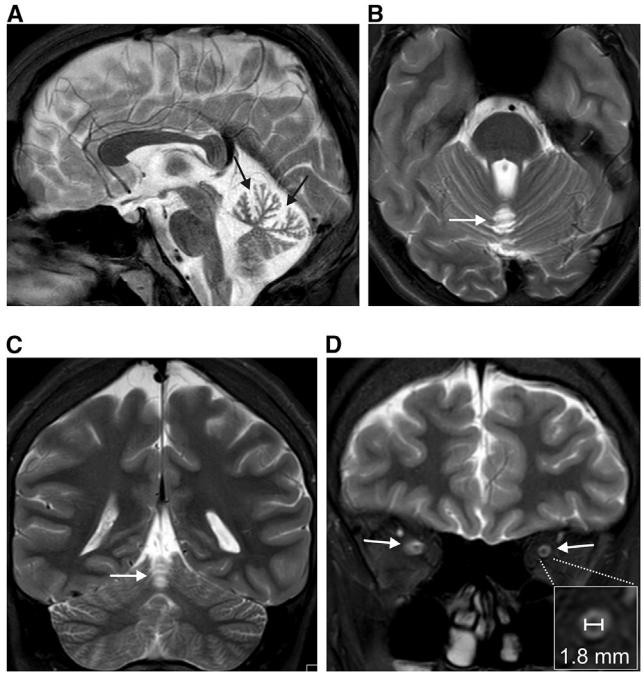

Figure 2. Selective Atrophy of the Cerebellar Vermis and Thinning of the Optic Nerve
(A–C) T2 weighted MRI scans from the male affected individual (F1:II.3) at age 16, revealing selective cerebellar vermis atrophy with spared hemispheres (and no brain stem or cerebral abnormalities). The signal of the cerebellar white and gray matter appears normal. Mid-sagittal cut showing upper vermis atrophy with markedly dilated interfolial fissures (black arrows) and normal pons (A), axial image (B), and coronal image (C) (note the normal hemispheres at this level). White arrows in (B) and (C) point to atrophic vermis.
(D) Retro-bulbar coronal cut from T2 weighted MRI scan from the same affected individual, showing optic nerve thinning (optic nerves are indicated by white arrows, the inset shows a close-up of transverse-cut optic nerve with a horizontal diameter of 1.8 mm). Significant optic nerve thinning as revealed by retro-bulbar diameter measurements was present in both affected siblings (1.7–1.9 mm, compared to ~3 mm in healthy age-matched probands[12]).

SureSelect XT2 All Exon V4 kit (Agilent). Sequencing (100 bp paired-end reads) was performed by GeneDx on a HiSeq 2000 sequencing system (Illumina). The DNA sequence was mapped to and analyzed against the reference human genome (UCSC Genome Browser hg19; within the targeted coding exons and splice junctions of known protein-coding RefSeq genes, the average depth-of-coverage was 119-fold and 97.8% of the target sequence was covered at least 10-fold). The GeneDx Xome Analyzer software was used to evaluate sequence changes in the affected individual in comparison to changes in other sequenced family members.

Whole-exome variant analysis did not yield pathogenic variants in any genes with known ataxia associations, neither in genes currently related to "hereditary ataxia" or in any of the 125 genes associated with "ataxia" in Human Gene Mutation Database (HGMD) entries. However, both affected siblings were found to harbor two mutations within *SCYL1* (SCY1-like, kinase-like [MIM: 607982]), c.937delG (p.Val313Cysfs*6) in exon 7 and c.1509_1510delTG (p.Ala504Profs*15) in exon 11 (GenBank: NM_020680.3). Neither mutation is represented in large reference datasets, such as 1000 Genomes (October 2014 data release, more than 2,500 individuals), the NHLBI Exome Sequencing Project (ESP) Exome Variant Server (6,500 exomes), or the Exome Aggregation Consortium Browser (ExAc, January 2015 release, encompassing data from more than 60,000 unrelated individuals). *SCYL1* mutations in all members of the family were confirmed by PCR and conventional DNA sequencing (PCR protocol and primer sequences are available from the authors on request).

The existence of two very rare putative null-mutations in *SCYL1*, the ortholog of which has been shown to be mutated in the *Scyl1*$^{mdf/mdf}$ mouse model,[5] provided strong evidence that disruption of *SCYL1* might be the molecular cause of the multisystem disorder in this family. In line with this assumption, we confirmed that both affected siblings are compound heterozygous for the two mutations, whereas both parents are carriers of only one or the other mutation and an unaffected sibling carries neither (Figures 3A–3C).

To determine whether disruptive mutations in *SCYL1* are causatively related to an autosomal recessively

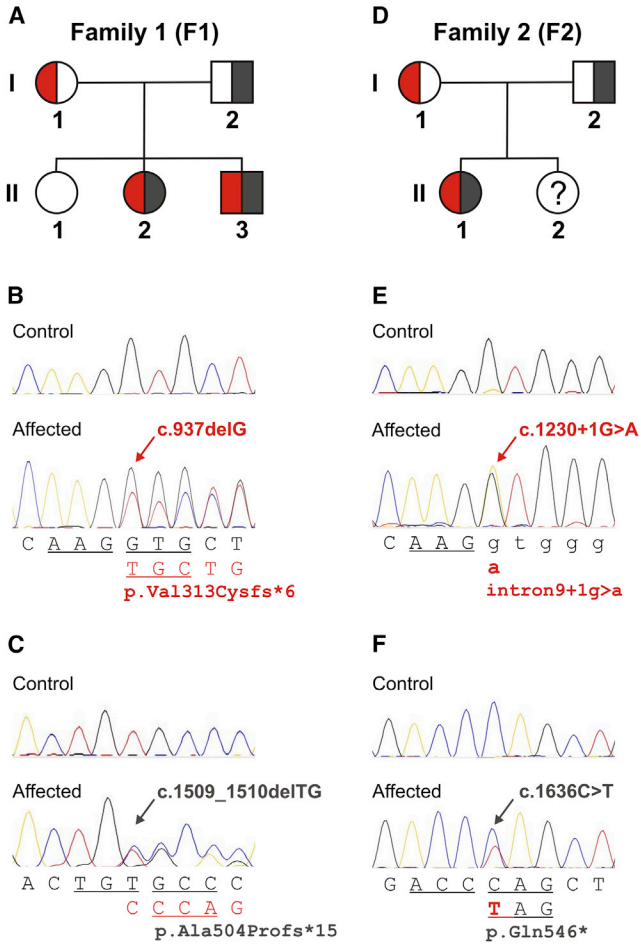

Figure 3. Compound Heterozygous *SCYL1* Mutations in Three Individuals from Two Unrelated Families

Panels (A)–(C) show family 1 and panels (D)–(F) show family 2. Pedigrees in (A) and (D) depict segregation of *SCYL1* lesions detected by whole-exome sequencing and confirmed by conventional capillary DNA sequencing (B and C and E and F, respectively). DNA from the unaffected sister in family 2 (F2:II.2) was not available for analysis. Biallelic mutations are represented in red and dark gray. Reference sequences are shown below the traces from affected individuals, where consequences caused by the respective mutations (indicated by arrows) are shown in the second lines. Codon triplets are represented by underlined letters, exonic residues are shown in capitals, and intronic sequence is shown in lower case. Mutation positions refer to GenBank transcript NM_020680.3.

inherited hepatocerebellar ataxia-neuropathy syndrome, we subsequently queried the Genesis (formerly GEM.app) database,[16] a collaborative web-platform comprising more than 7,000 whole exomes and 1,200 whole genomes, including ~5,000 datasets of families with a wide spectrum of neurological disorders. Whole-exome sequencing was performed with the SureSelect Human All Exon 50Mb kit (Agilent) for capture and 120 bp paired-end sequencing on a HiSeq2000 (Illumina). Data analysis was performed with the Genesis (GEM.app) pipeline (the average depth-of-coverage was 77-fold and 85% of the target sequence was covered at least 10-fold).

We identified two different formally disruptive *SCYL1* mutations in a presently 17-year-old girl (F2:II.1, Table 1) initially diagnosed with Charcot-Marie-Tooth disease. The phenotype bore striking similarities to the two siblings with *SCYL1* mutations described above. The girl was born to non-consanguineous parents with at least three generations of Cuban family history (family 2). Between the ages of 18 months and 3 years, she suffered from three episodes of acute liver failure, each brought about by a febrile infection, which left hepatosplenomegaly as a residuum. Liver biopsy performed during one of the acute episodes revealed acute hepatitis with early bridging fibrosis. The first of these episodes was accompanied by a generalized status epilepticus and required artificial respiration for almost three weeks. Although her achievements of motor milestones were reportedly normal, she developed progressive gait problems at age 3, leading to frequent falling and early exhaustion, and a progressively debilitating neurogenic stutter. At age 10, running was barely possible and markedly reduced fine motor coordination was noted. At age 17, a predominant motor peripheral neuropathy, manifested by distally accentuated weakness in the upper and lower limbs, pronounced amyotrophy of the hands and feet, and bilateral pes equinus, dominated the clinical picture. Additionally, mild cerebellar and pyramidal system involvement was noted and a learning disability suspected, although not formally tested. Nerve conduction studies corroborated the diagnosis of a mixed sensorimotor peripheral neuropathy. At age 13, a subtle atrophy of the upper cerebellar vermis was noted on MRI (Figure S1). Measurements of optic nerve diameters were not possible for technical reasons.

The *SCYL1* mutations identified in this individual, namely a splice-site mutation (c.1230+1G>A [p.?]) affecting the invariable +1 nucleotide of intron 9 (causing disruption of correct mRNA splicing by inducing skipping of exon 9, which encodes part of the HEAT repeat domain, Figure S2) and a premature termination mutation (c.1636C>T [p. Gln546*]) in exon 12, are predictably deleterious. Neither mutation is referred to in the reference databases mentioned above. Whereas the mother (F2:I.1) is heterozygous for the splice-site mutation, the father (F2:I.2) is heterozygous for the nonsense mutation, indicating compound heterozygosity (Figures 3D–3F).

In the next step, we probed dermal fibroblasts of the affected individuals and their parents (family 1) to determine the amounts of SCYL1 by using two antibodies directed against the C and N termini of SCYL1.[5] In contrast to the normal amount of SCYL1 detected in fibroblasts from both parents, there was a complete loss of SCYL1 in fibroblasts from both affected individuals, as revealed by western blotting (Figure 4A) and immunofluorescence experiments (Figures 4B and 4C).

SCYL1-knockdown in vitro experiments in HeLa cells suggested a role of SCYL1 in context with the integrity of the Golgi apparatus.[8,9] Therefore, we measured the surface area of the Golgi in dermal fibroblasts derived from

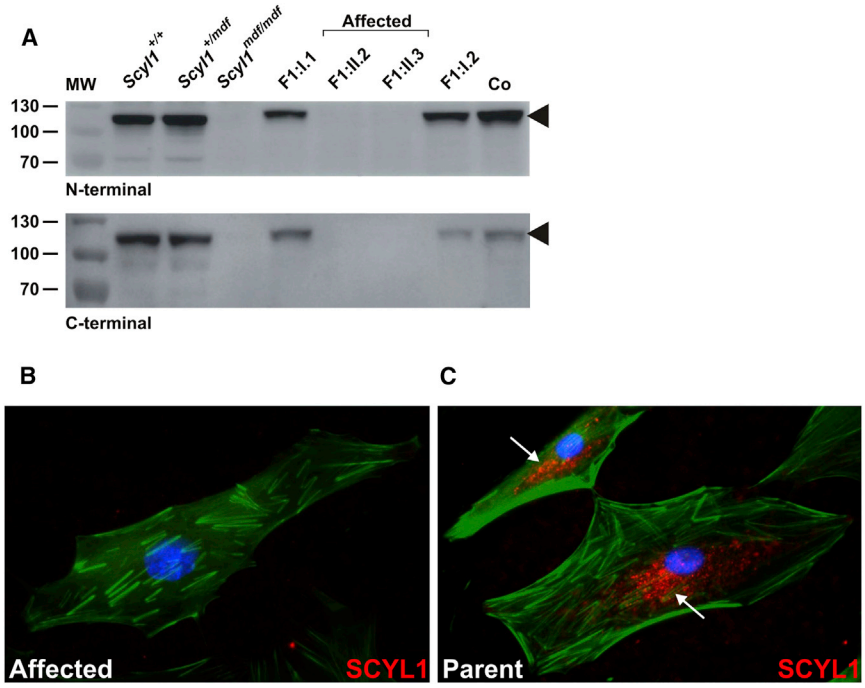

Figure 4. *SCYL1*-Null Mutations Lead to Complete Lack of SCYL1 in Cultured Skin Fibroblasts

(A) Complete loss of SCYL1 in protein extracts from fibroblasts from both affected siblings (F1:II.2 and F1:II.3), in contrast to fibroblasts from their parents (F1:I.1 and F1:I.2), with both N-terminal (upper panel) and C-terminal antibodies (lower panel). Extracts prepared from human WI-38 fetal lung fibroblasts (Co) and murine fibroblasts from *mdf* (*Scyl1*$^{mdf/mdf}$) and wild-type (*Scyl1*$^{+/+}$) as well as heterozygous (*Scyl1*$^{+/mdf}$) littermates were used as controls. MW; molecular weight marker (kDa). Arrowheads indicate full-length SCYL1 (~105 kDa band).

(B and C) Absent SCYL1 immunoreactivity (N-terminal antibody, goat anti-rabbit secondary antibody conjugated with Alexa Fluor 594, red fluorescence) in skin fibroblasts from female affected individual F1:II.2 (B) in comparison to a predominantly perinuclear vesicular SCYL1-staining pattern (white arrows) obtained in fibroblasts from her mother, F1:I.1 (C). The F-actin cytoskeleton is visualized by Phalloidin Atto 488 (green fluorescence) and nuclei are depicted with DAPI (blue).

affected individuals and their parents and found the Golgi to be massively enlarged in SCYL1-negative cells (Figures 5A–5C). These data indicate that SCYL1 is indeed a regulator of Golgi morphology not only in HeLa cells in knockdown experiments,[9] but also in primary human fibroblasts affected by naturally occurring, disruptive mutations of *SCYL1*.

The clinical manifestations of the disease in the individuals described in this study overlap to a large extent with the phenotype of the *Scyl1*$^{mdf/mdf}$ mouse model. Cerebellar ataxia accompanied by cerebellar vermis atrophy, motor-predominant peripheral neuropathy, and optic-nerve thinning are consistent neurological features in both mice and humans. Whereas peripheral neuropathy and distal muscular atrophy predominate in individual F2:II.1, cerebellar ataxia represents the most striking phenotype in both siblings in family 1 (F1:II.2 and F1:II.3). However, neurogenic stuttering, optic-nerve thinning and upper motor neuron dysfunction suggest a more widespread SCYL1-associated clinical and pathologic phenotype. Intriguingly, although all three affected individuals reported here presented with severe recurrent episodes of acute liver failure in infancy, no such episodes or corresponding phenotypes have been observed in the *Scyl1*$^{mdf/mdf}$ mouse so far, warranting more in-depth investigations regarding this in the mouse model.

Collectively, our data provide compelling evidence that disruptive mutations in *SCYL1* cause a syndrome characterized by early-onset episodes of acute liver failure, cerebellar ataxia, and peripheral motor and sensory neuropathy in humans. It is probable that the *SCYL1* mutations identified here represent the more severe end of the mutational landscape. Other lesions, such as missense mutations, which do not fully abrogate SCYL1 function, might be associated with a variable clinical picture. The description of other individuals with *SCYL1* mutations has to be awaited, which will allow the capture of a foreseeably-wide clinical spectrum of manifestations. Our findings add *SCYL1* to a list of several other genes implicated in disorders involving the cerebellum, whose gene products are implicated in the Golgi network.[17–19]

Several causes for hereditary infantile liver failure are currently known. Interestingly, mutations in *MARS* (MIM: 156560) and *LARS* (MIM: 151350), both encoding tRNA synthetases, are associated with multisystem manifestations involving transient infantile hepatopathy.[20,21] Although speculative, the functional role of SCYL1 in nuclear-cytoplasmic tRNA transport might therefore be related to the molecular mechanism behind the transient liver failure shared by all three individuals with *SCYL1* mutations in this study. Notably, mutations in *NBAS* (MIM: 608025), encoding a protein that is apparently involved in retrograde transport from the Golgi to the ER, were recently shown to cause early-onset recurrent acute liver failure (infantile liver failure syndrome 2, ILFS2 [MIM: 616483])[22] or a multisystem disorder involving infantile liver failure.[23] Because SCYL1 was also shown to be involved in a similar Golgi-ER-pathway,[10] it is tempting to speculate that dysfunction of the Golgi-ER transport function might represent a common pathogenic mechanism, which underlies severe recurrent episodes of acute liver failure in infancy. These parallels warrant further studies to investigate how loss of SCYL1 can cause liver failure.

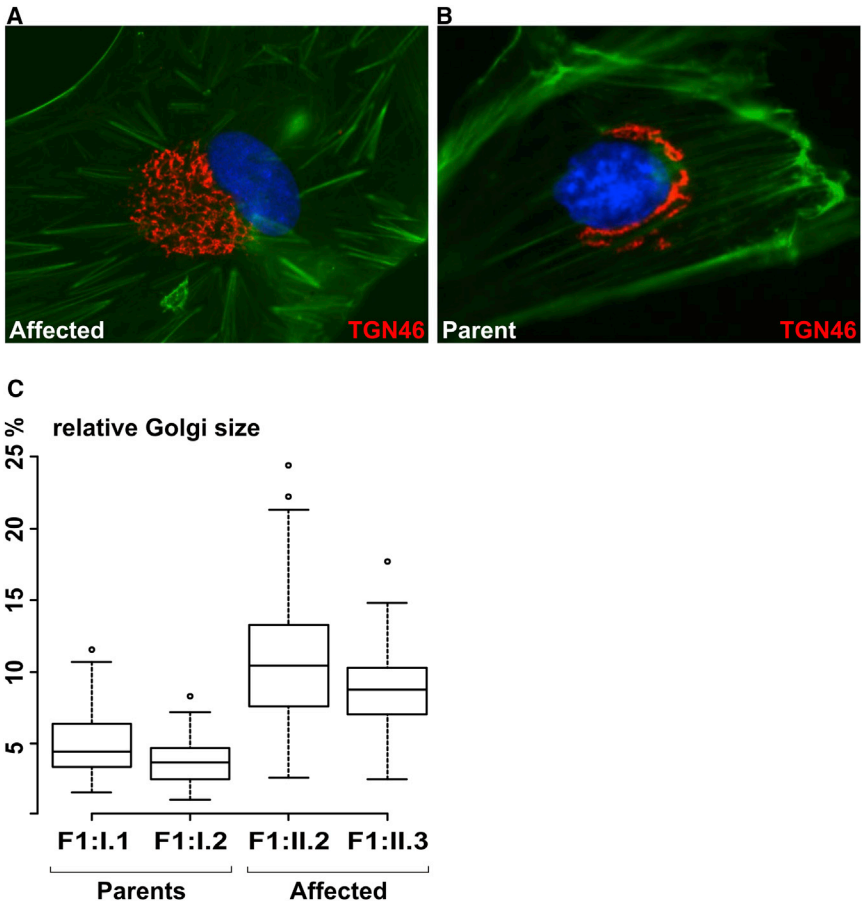

Figure 5. Absence of SCYL1 Leads to Enlargement of the Golgi Apparatus in Human Fibroblasts

By immunofluorescence, the Golgi network appeared enlarged in the skin fibroblasts from the male affected individual, F1:II.3, (A) when compared to the Golgi staining in his father's, F1:I.2, fibroblasts (B). Anti-TGN46 (also known as TGOLN2, a trans-Golgi-network protein) antibody (Sigma-Aldrich; T7576) is shown as red fluorescence. The F-actin cytoskeleton is visualized by Phalloidin Atto 488 (green fluorescence) and nuclei are depicted with DAPI (blue). Morphometric analysis revealed enlargement of Golgi apparatuses in SCYL1-negative fibroblasts (C). Shown as a percentage of total cell size; $p < 5e\text{-}14$, Mann-Whitney-Wilcoxon test.

Once more, this study demonstrates that molecular genetics and pre-clinical research on mouse models is capable of propelling the identification and understanding of the corresponding human disease[24,25] and strongly argues for an unbiased exome-wide strategy in the molecular diagnosis of individuals affected by rare inherited disorders.

Supplemental Data

Supplemental Data include two figures and can be found with this article online at http://dx.doi.org/10.1016/j.ajhg.2015.10.011.

Acknowledgments

The authors are grateful for the participation of the affected individuals and their parents in this study. The authors thank David R. Kelly, M.D. (Pathologist-in-Chief and Medical Director of Laboratories, Children's of Alabama, Birmingham, AL and Clinical Professor of Pathology, University of Alabama at Birmingham) for pathological expertise, Lisa Abreu, Feifei Tao, and Cima Saghira (Hussman Institute for Human Genomics, University of Miami) for coordination of clinical data collection and assistance in molecular genetic analysis, and Jennifer Reichbauer (Hertie Institute for Clinical Brain Research, University of Tübingen) for RNA analysis in family 2. The authors thank Ludger Schöls, M.D. (Hertie-Institute for Clinical Brain Research and German Research Center for Neurodegenerative Diseases) for establishing the research cooperation that finally led to identification of the third individual with *SCYL1* mutations. This study was supported by the Interdisciplinary Center for Clinical Research Tübingen (grant 1970-0-0 to R.S.), the European Union (grant PIOF-GA-2012-326681 "HSP/CMT genetics" to R.S.), E-RARE grants of the German Ministry for Education and Research to the NEUROLIPID project (01GM1408B to R.S.), and the NIH (grants 5R01NS072248, 1R01NS075764, and 5R01NS054132 to S.Z.).

Received: September 17, 2015
Accepted: October 16, 2015
Published: November 12, 2015

Web Resources

The URLs for data presented herein are as follows:

1000 Genomes, http://browser.1000genomes.org
ExAC Browser, http://exac.broadinstitute.org/
GenBank, http://www.ncbi.nlm.nih.gov/genbank/
HGMD Professional, http://www.biobase-international.com/product/hgmd
NHLBI Exome Sequencing Project (ESP) Exome Variant Server, http://evs.gs.washington.edu/EVS/
OMIM, http://www.omim.org/
UCSC Genome Browser, http://genome.ucsc.edu

References

1. Storey, E. (2014). Genetic cerebellar ataxias. Semin. Neurol. *34*, 280–292.

2. Mancuso, M., Orsucci, D., Siciliano, G., and Bonuccelli, U. (2014). The genetics of ataxia: through the labyrinth of the Minotaur, looking for Ariadne's thread. J. Neurol. *261*, S528–S541.
3. Jayadev, S., and Bird, T.D. (2013). Hereditary ataxias: overview. Genet. Med. *15*, 673–683.
4. Anheim, M., Tranchant, C., and Koenig, M. (2012). The autosomal recessive cerebellar ataxias. N. Engl. J. Med. *366*, 636–646.
5. Schmidt, W.M., Kraus, C., Höger, H., Hochmeister, S., Oberndorfer, F., Branka, M., Bingemann, S., Lassmann, H., Müller, M., Macedo-Souza, L.I., et al. (2007). Mutation in the Scyl1 gene encoding amino-terminal kinase-like protein causes a recessive form of spinocerebellar neurodegeneration. EMBO Rep. *8*, 691–697.
6. Blot, S., Poirier, C., and Dreyfus, P.A. (1995). The mouse mutation muscle deficient (mdf) is characterized by a progressive motoneuron disease. J. Neuropathol. Exp. Neurol. *54*, 812–825.
7. Liu, S.C., Lane, W.S., and Lienhard, G.E. (2000). Cloning and preliminary characterization of a 105 kDa protein with an N-terminal kinase-like domain. Biochim. Biophys. Acta *1517*, 148–152.
8. Hamlin, J.N., Schroeder, L.K., Fotouhi, M., Dokainish, H., Ioannou, M.S., Girard, M., Summerfeldt, N., Melançon, P., and McPherson, P.S. (2014). Scyl1 scaffolds class II Arfs to specific subcomplexes of coatomer through the γ-COP appendage domain. J. Cell Sci. *127*, 1454–1463.
9. Burman, J.L., Hamlin, J.N., and McPherson, P.S. (2010). Scyl1 regulates Golgi morphology. PLoS ONE *5*, e9537.
10. Burman, J.L., Bourbonniere, L., Philie, J., Stroh, T., Dejgaard, S.Y., Presley, J.F., and McPherson, P.S. (2008). Scyl1, mutated in a recessive form of spinocerebellar neurodegeneration, regulates COPI-mediated retrograde traffic. J. Biol. Chem. *283*, 22774–22786.
11. Chafe, S.C., and Mangroo, D. (2010). Scyl1 facilitates nuclear tRNA export in mammalian cells by acting at the nuclear pore complex. Mol. Biol. Cell *21*, 2483–2499.
12. Lenhart, P.D., Desai, N.K., Bruce, B.B., Hutchinson, A.K., and Lambert, S.R. (2014). The role of magnetic resonance imaging in diagnosing optic nerve hypoplasia. Am. J. Ophthalmol. *158*, 1164–1171.
13. Pyle, A., Smertenko, T., Bargiela, D., Griffin, H., Duff, J., Appleton, M., Douroudis, K., Pfeffer, G., Santibanez-Koref, M., Eglon, G., et al. (2015). Exome sequencing in undiagnosed inherited and sporadic ataxias. Brain *138*, 276–283.
14. Ng, S.B., Buckingham, K.J., Lee, C., Bigham, A.W., Tabor, H.K., Dent, K.M., Huff, C.D., Shannon, P.T., Jabs, E.W., Nickerson, D.A., et al. (2010). Exome sequencing identifies the cause of a mendelian disorder. Nat. Genet. *42*, 30–35.
15. Choi, M., Scholl, U.I., Ji, W., Liu, T., Tikhonova, I.R., Zumbo, P., Nayir, A., Bakkaloğlu, A., Ozen, S., Sanjad, S., et al. (2009). Genetic diagnosis by whole exome capture and massively parallel DNA sequencing. Proc. Natl. Acad. Sci. USA *106*, 19096–19101.
16. Gonzalez, M., Falk, M.J., Gai, X., Postrel, R., Schüle, R., and Zuchner, S. (2015). Innovative Genomic Collaboration Using the GENESIS (GEM.app) Platform. Hum. Mutat. *36*, 950–956.
17. Di Gregorio, E., Borroni, B., Giorgio, E., Lacerenza, D., Ferrero, M., Lo Buono, N., Ragusa, N., Mancini, C., Gaussen, M., Calcia, A., et al. (2014). ELOVL5 mutations cause spinocerebellar ataxia 38. Am. J. Hum. Genet. *95*, 209–217.
18. Corbett, M.A., Schwake, M., Bahlo, M., Dibbens, L.M., Lin, M., Gandolfo, L.C., Vears, D.F., O'Sullivan, J.D., Robertson, T., Bayly, M.A., et al. (2011). A mutation in the Golgi Qb-SNARE gene GOSR2 causes progressive myoclonus epilepsy with early ataxia. Am. J. Hum. Genet. *88*, 657–663.
19. Senderek, J., Krieger, M., Stendel, C., Bergmann, C., Moser, M., Breitbach-Faller, N., Rudnik-Schöneborn, S., Blaschek, A., Wolf, N.I., Harting, I., et al. (2005). Mutations in SIL1 cause Marinesco-Sjögren syndrome, a cerebellar ataxia with cataract and myopathy. Nat. Genet. *37*, 1312–1314.
20. van Meel, E., Wegner, D.J., Cliften, P., Willing, M.C., White, F.V., Kornfeld, S., and Cole, F.S. (2013). Rare recessive loss-of-function methionyl-tRNA synthetase mutations presenting as a multi-organ phenotype. BMC Med. Genet. *14*, 106.
21. Casey, J.P., McGettigan, P., Lynam-Lennon, N., McDermott, M., Regan, R., Conroy, J., Bourke, B., O'Sullivan, J., Crushell, E., Lynch, S., and Ennis, S. (2012). Identification of a mutation in LARS as a novel cause of infantile hepatopathy. Mol. Genet. Metab. *106*, 351–358.
22. Haack, T.B., Staufner, C., Köpke, M.G., Straub, B.K., Kölker, S., Thiel, C., Freisinger, P., Baric, I., McKiernan, P.J., Dikow, N., et al. (2015). Biallelic Mutations in NBAS Cause Recurrent Acute Liver Failure with Onset in Infancy. Am. J. Hum. Genet. *97*, 163–169.
23. Garcia Segarra, N., Ballhausen, D., Crawford, H., Perreau, M., Campos-Xavier, B., van Spaendonck-Zwarts, K., Vermeer, C., Russo, M., Zambelli, P.Y., Stevenson, B., et al. (2015). NBAS mutations cause a multisystem disorder involving bone, connective tissue, liver, immune system, and retina. Am. J. Med. Genet. A. Published online August 19, 2015. http://dx.doi.org/10.1002/ajmg.a.37338.
24. Longman, C., Brockington, M., Torelli, S., Jimenez-Mallebrera, C., Kennedy, C., Khalil, N., Feng, L., Saran, R.K., Voit, T., Merlini, L., et al. (2003). Mutations in the human LARGE gene cause MDC1D, a novel form of congenital muscular dystrophy with severe mental retardation and abnormal glycosylation of alpha-dystroglycan. Hum. Mol. Genet. *12*, 2853–2861.
25. Grewal, P.K., Holzfeind, P.J., Bittner, R.E., and Hewitt, J.E. (2001). Mutant glycosyltransferase and altered glycosylation of alpha-dystroglycan in the myodystrophy mouse. Nat. Genet. *28*, 151–154.